Biochimica et Biophysica Acta, 375 (1975) 69–86

BBA 76839

MAGNETIC RESONANCE STUDIES OF THE MITOCHONDRIAL DIVALENT CATION CARRIER

GEORGE D. CASE*

Department of Biophysics and Physical Biochemistry, Johnson Research Foundation, The School of Medicine, University of Pennsylvania, Philadelphia, Pa. 19174 (U.S.A.)

(Received April 5th, 1974)
(Revised manuscript received September 19th, 1974)

SUMMARY

Measurements of water proton spin relaxation enhancements (ε) can be used to discriminate high-affinity binding of Mn^{2+} or Gd^{3+} to biological membranes, from low-affinity binding. In rat liver mitochondria, ε_b values of approx. 11 are observed upon binding of Mn^{2+} to the inner membrane, while internal or low-affinity binding remains invisible to this technique. Energy-driven Mn^{2+} uptake by liver mitochondria results in the subsequent decay of ε^*.

Comparison of ε^* with the initial velocity of Mn^{2+} uptake in rat liver mitochondria reveals a linear correlation, which holds at all temperatures between 0 °C and 40 °C, regardless of the mitochondrial protein concentration. Consequently, enhancement appears to reflect the binding of Mn^{2+} to the divalent cation pump.

Binding of Mn^{2+} to blowfly flight muscle also results in substantial ε^*, which is associated with the glycerol-1-phosphate dehydrogenase instead of divalent cation transport. Consequently, no decay in ε^* due to uptake occurs after Mn^{2+} is bound.

Lanthanide ions are also bound and transported by mitochondria. Addition of Gd^{3+} to pigeon heart or rat liver mitochondria results in $\varepsilon_b \approx 5$–6, which decays with similar kinetics in both systems. The uptake velocity of Gd^{3+} in rat liver mitochondria is about 1/6 the rate with which Mn^{2+} is transported. Lanthanides also diminish ε^* due to the addition of Mn^{2+}, and greatly retard the Mn^{2+} uptake kinetics. The presence of carbonylcyanide-*p*-trifluoromethoxyphenylhydrazone depresses ε^* upon addition of Mn^{2+} or Gd^{3+} and also uncouples energy-driven uptake. On the other hand, prolonged anaerobic incubation in the presence of antimycin and rotenone exhausts the mitochondria of their energy stores, blocks the uptake of Mn^{2+}, but does not affect ε^* significantly. Evidently, the uncoupler-induced disappearance of divalent cation binding sites is not the result of "de-energization".

Measurements of ε^* at several NMR frequencies indicate a correlation time (τ_b) for carrier-bound Mn^{2+} in rat liver mitochondria between 20 ns and 4 ns as one varies the temperature between 10 °C and 30 °C. The 13 Kcal/mole activation energy

* Present address: Department of Physiology-Anatomy, University of California, Berkeley, California 94720, U.S.A.

for τ_b suggests that the 11 ns time constant at room temperature represents the movement of the Mn^{II}–carrier complex. On the other hand, τ_b is probably approx. 100 times too short to represent the rotational motion of a carrier protein. Apparently, Mn^{2+} binds to a small arm of the carrier which moves independently of the main body of any protein.

In addition to $Mn(H_2O)_6^{2+}$, other complexes of Mn^{2+} may also be bound and transported by rat liver mitochondria. Only a small increase in ε^* occurs upon addition of $MnHPO_4$, yet this species is accumulated by the mitochondria. Consequently, the carrier does not recognize divalent metal ions on the basis of charge.

INTRODUCTION

The energy-dependent transport of Ca^{2+} and other divalent cations across the inner mitochondrial membrane has been discussed extensively [1–3]. Divalent cation uptake can be driven by coupled respiration, coupled ATP hydrolysis, or by energy stored in electrochemical gradients [1–4]. The "uphill" direction of divalent cation transport [1, 4, 5] and also its sensitivity to La^{3+}, which blocks transport without adversely affecting oxidative phosphorylation [6], have led some investigators to postulate the existence of a special carrier [6, 7]. According to Mela and Chance [6], the very low concentration of La^{3+} required for inhibition (< 0.1 nmole/mg protein) suggests that the rare earth binds specifically to the carrier. Recent evidence by Vinogradov and Scarpa [8] indicates that divalent cation uptake exhibits sigmoidal kinetics, suggesting that cooperativity may be involved in the process. This result would strongly support a model of carrier-mediated transport in mitochondria which requires binding of at least 2 divalent ions. However, these studies can provide only indirect information regarding the mechanism of transport.

A more direct approach to studies of the divalent cation carrier involves the use of suitable NMR and EPR techniques to follow interactions with a paramagnetic cation such as Mn^{2+} [2]. Recent EPR experiments [5, 9, 10] have suggested that $Mn(H_2O)_6^{2+}$ is accumulated in the matrix space under massive loading conditions in the presence of acetate, and $MnHPO_4$ under similar conditions in the presence of phosphate. A broadened spectrum which these authors [5, 9, 10] attributed to a bound form of Mn(II) was also observed. However, no identification of the binding sites in the mitochondria was reported.

In 1963, Chappell et al. [2] described the use of a pulsed-NMR technique to monitor Mn^{2+} uptake in mitochondria. The relaxation rate ($1/T_1$) of the water protons is accelerated in the presence of certain paramagnetic ions, in which the increment [11–14]

$$\frac{1}{T_{1p}} = \frac{[H_2O]_p}{T_{1M}+\tau_m} \approx \frac{[H_2O]_p}{T_{1M}} \tag{1}$$

Here, $[H_2O]_p$ is the mole fraction of water in the Mn^{2+} coordination sphere; T_{1M} is the NMR relaxation time of these particular water molecules; and τ_m is the water residence time. The binding of aqueous Mn^{2+} to a large ligand such as a protein frequently results in an enhanced acceleration of the relaxation rate [11], in which case the enhancement

$$\varepsilon \equiv \frac{(1/T_{1p})_{bound}}{(1/T_{1p})_{free}} \tag{2}$$

The rotational mobility of the paramagnetic center, electron relaxation rates of the ion, and the degree of displacement of the coordination water molecules are factors which govern ε [11–14].

In the absence of a diffusion barrier, the perturbation of the relaxation rate by Mn^{2+} is transmitted throughout the bulk solution because the rate of water proton exchange is much faster than $1/T_{1M}$ [11–14]. However, the presence of a membrane can exert a profound influence, since the permeability of H_2O ($\tau \approx 5$ ms for erythrocyte ghosts [15]) is very likely several orders of magnitude slower than T_{1M} (which is ≈ 0.1–1.0 μs [11]). If mitochondrial membranes are similarly resistant to H_2O diffusion, then the internal spaces of the particles should be invisible to this technique. Consequently, Mn^{2+} should perturb the proton relaxation times of H_2O only while it remains in contact with the outside of the vesicle; and uptake of the ion by mitochondria should result in a decrease in enhancement.

Proton relaxation enhancement measurements have been successful in soluble enzyme systems [11], and have revealed important clues about active site structure and catalytic mechanisms. In mitochondria, Chappell et al. [2] reported values of $\varepsilon^* =$ 5–7 for Mn^{2+} surface binding, and lower values of ε^* for Mn^{2+} bound to a second class of sites. In light of the relative impermeability of the mitochondrial inner membrane to H_2O, these sites might correspond to high-affinity and low-affinity, as opposed to external and internal, binding sites. On the other hand, the number of high-ε^* sites which Chappell et al. [2] observed was about 20 times greater than the number of high-affinity sites reported by Reynafarje and Lehninger [7], and 300–600 times the number of La^{3+}-sensitive "carrier" sites [4, 6].

The present report examines some properties of mitochondrial high-affinity cation binding in an attempt to evaluate its functional role. We shall clarify the early experiments of Chappell et al. [2] and demonstrate a connection between the NMR relaxation enhancement and Mn^{2+} binding to the carrier. This work also investigates some of the physical properties of the Mn (II) carrier complex and explores certain aspects of the transport mechanism which have not been resolved by more classical techniques. A portion of this work has been discussed previously [16].

EXPERIMENTAL

All inorganic and organic chemicals were reagent grade and were used without further purification. Carbonylcyanide-*p*-trifluoromethoxyphenylhydrazone (FCCP) was obtained from Calbiochem. Antimycin *a* was procured from Sigma and rotenone was purchased from K and K Labs. The antibiotic A23187 [17, 18] was the generous gift of Dr Robert Hamill, Eli Lilly Co., Indianapolis, Indiana. Flight muscle mitochondria from blowflies (*Phormia regina*) were generously provided by Dr Richard G. Hansford, Gerontology Research Center, National Institutes of Health, Baltimore, Maryland [19]. Preparation of mitochondria from rat liver [20], *Saccharomyces cervisciae* [21] and pigeon heart [22] followed standard procedures. Sarcoplasmic reticulum vesicles were isolated from rabbit skeletal muscle according to the method of McFarland and Inesi [23], and chromatophores from *Rhodopseudomonas spher-*

oides, according to previously described methods [24]. Protein content was determined by means of the biuret assay [25].

For some experiments (Figs 6 and 7), Ca^{2+} and Mn^{2+} transport were followed spectrophotometrically at 540–507 nm with the indicator murexide [26, 27]. Alternatively, Mn^{2+} and Gd^{3+} were determined by magnetic resonance techniques. EPR measurements were carried out on a Varian E4 spectrometer, and the spectra were averaged and integrated on a Nicolet 1074 computer. Spin-echo measurements of ^1H_2O proton NMR relaxation rates were carried out on a pulsed NMR instrument described by Cohn [28]. Temperature regulation was achieved with either a Haake bath or with a Varian air-circulated controller, and the temperature of the samples was measured intermittently with a Tri-R electronic thermometer.

RESULTS

High affinity binding and the divalent cation carrier

Fig. 1 presents some typical ^1H_2O proton relaxation measurements of the binding and transport of Mn^{2+} and Gd^{3+} in mitochondria under limited loading conditions. Immediately upon addition of Mn^{2+}, ε^* increases to a value between 5 and 7. Separate experiments with higher protein concentrations give $\varepsilon^* \approx 11$, in mitochondria from either rat liver or blowfly flight muscle. Similar additions of Gd^{3+} to mitochondria (in place of Mn^{2+}) elicit ε^* values which are somewhat smaller

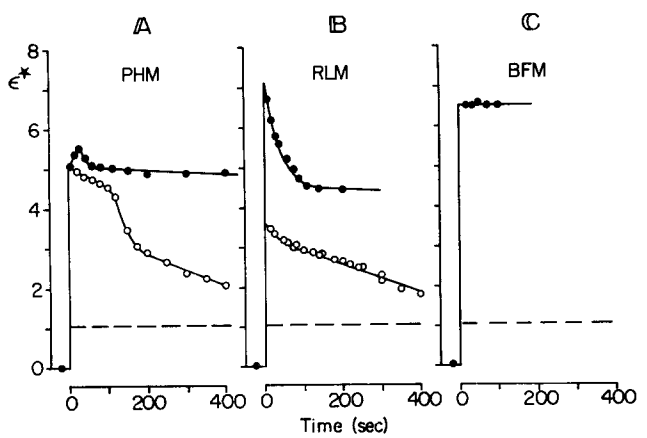

Fig. 1. Proton relaxation enhancement and Mn^{2+} transport in mitochondria from pigeon heart, rat liver, and blowfly flight muscle. T_1 of the mitochondrial suspension was measured at an NMR frequency of 24.3 MHz before and at various times after the addition of 100 μM $MnCl_2$ (- ● -) or 100 μM $GdCl_3$ (- ○ -). The effect of the Mn^{2+} addition on the T_1 of pure medium is expressed as the horizontal dashed line at $\varepsilon^* = 1$, and is time-independent. A. Pigeon heart mitochondria (PHM), 12 mg protein/ml. Medium consisted of 0.3 M mannitol, 0.02 M potasssium morpholinopropane sulfonate buffer, 5 mM sodium glutamate, and 10 mM sodium succinate, pH 7.4. B. Rat liver mitochondria (RLM), 9 mg protein/ml. Medium consisted of 0.3 M sucrose, 0.02 M potassium morpholinopropane sulfonate buffer, 5 mM monosodium glutamate, and 10 mM sodium potassium succinate, pH 7.4. C. Blowfly flight muscle (BFM) mitochondria, 16 mg protein/ml. Medium consisted of 0.3 M sucrose, 5 mM sodium tris(hydroxymethyl) aminomethane ethanesulfonate buffer, 5 mM sodium pyruvate, and 10 mM proline, pH 7.4 (see ref. 30).

(Figs 1A, 1B). As Mn^{2+} is taken up into the rat liver mitochondrial matrix, ε^* decays to a final value which is approximately $\frac{1}{2}$ of its original level (Fig. 1B). A23187 allows Mn^{2+} to leak from the matrix, but does not affect the binding of Mn^{2+} to sites on the membrane (Fig. 4A). Larger additions of Mn^{2+} to rat liver mitochondrial suspensions increase the extent of uptake without increasing the initial velocity of uptake or the initial ε^*.

No decay in ε^* subsequent to the addition of Mn^{2+} is seen in pigeon heart mitochondria or blowfly mitochondria (Figs 1A, 1C), since these preparations do not actively transport divalent cations under the existing conditions [19]. Exposure of pigeon heart mitochondria to proteolytic digestion during preparation [22] apparently damages the divalent cation carrier because heart mitochondria prepared without this digestion step transport Ca^{2+} effectively [29]. One can argue, therefore, that the residual ε^* which is observed in Fig. 1A is due to the binding of Mn^{2+} to an accessory site which remains intact on the mitochondrial inner membrane.

On the other hand, no Mn^{2+} uptake occurs in blowfly mitochondria under limited loading conditions (Fig. 1C) because the M^{2+} carrier has a very low affinity for divalent ions [19]. Nevertheless, initial ε^* values between 6 and 7 are also observed in blowfly mitochondria. The data of Table I indicate that Mn^{2+} binds to a site which is specific for glycerol 1-phosphate, since this substrate depresses ε^* substantially, while other substrates do not lower ε^*. No substrate appears to stimulate M^{2+} transport in blowfly mitochondria at the low levels of Mn^{2+} used in the Fig. 1 experiment. Previous evidence [30] has shown that glycerol 1-phosphate-dependent respiration in blowfly mitochondria requires Ca^{2+}, with $K_D < 1$ μM. In this case, ε^* is attributed to the high-affinity binding of Mn^{2+} to the Ca^{2+} site on the glycerol-1-phosphate dehydrogenase. Contrarily, in mitochondria from pigeon heart or rat liver, the presence of glycerol 1-phosphate does not diminish the initial ε^*. Thus, Ca^{2+} or Mn^{2+} binding to a glycerol-1-phosphate dehydrogenase is visible only in mitochondria which functionally resemble the blowfly system.

Fig. 1 also shows the decay in ε^* which follows the addition of Gd^{3+} to rat liver or pigeon heart mitochondria. In similar experiments, subsequent addition of the ionophore A23187 reverses the decay in ε^*, while addition of ethanol accelerates it. Both observations support the view that Gd^{3+} is transported across the inner mitochondrial membrane in these systems. However, the data of Fig. 1 also strongly suggest that lanthanides traverse the membrane by a mode different from Ca^{2+} and Mn^{2+}, because Gd^{3+} uptake is observed in pigeon heart mitochondria with impaired Ca^{2+}/Mn^{2+} uptake (Fig. 1A, also ref. 29). Spectrophotometric measurements of

TABLE I

EFFECT OF SUBSTRATE BINDING TO BLOWFLY MITOCHONDRIA ON ε^*

Blowfly flight muscle mitochondria (16 mg protein/ml) were suspended in a medium containing 0.25 M sucrose and 5 mM sodium tris(hydroxymethyl)aminomethane ethanesulfonate, pH 7.4. Conditions otherwise as in Fig. 1C.

No substrate (ε^*)	10 mM glycerol 1-phosphate (ε^*)	5 mM pyruvate + 5 mM proline (ε^*)
7.5, 7.8	2.8	6.2

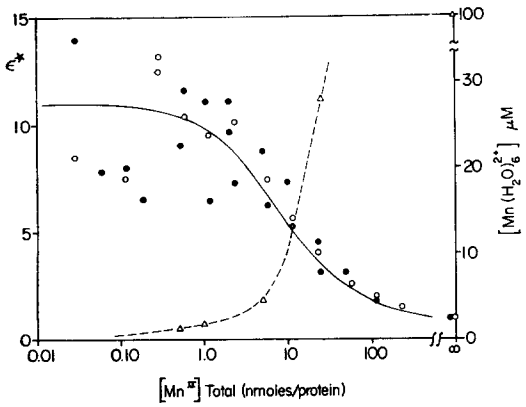

Fig. 2. Titration of ε^* in rat liver mitochondria. Conditions similar to those used in Fig. 1B, except that pH was 7.2, and no substrates were present. ε^* was determined by extrapolating T_1 back toward zero time. 100 μM $MnCl_2$ was added to suspensions of mitochondria which contained varying amounts of protein. However, at the lowest ratios of Mn^{2+} protein, smaller additions of Mn^{2+} were also employed in order to extend the titration by an order of magnitude. The abscissa represents the concentration of total Mn^{2+}. (Δ), EPR measurements of free aqueous Mn^{2+}, using the same samples as shown below for ε^* measurements; (●), no inhibitors; (○), 20 μg/ml antimycin and 1.5 μM rotenone present. Mitochondria incubated for >50 min at 0 °C and 5 min at 20 °C prior to measurement.

Gd^{3+} binding and transport, with the indicator murexide [26, 27], also show that Gd^{3+} is taken up from the bulk solution by pigeon heart mitochondria under conditions in which respiration is blocked by antimycin and rotenone, or uncoupled. Hence, no energy source appears necessary for lanthanide transport.

Fig. 2 shows titrations of ε^* due to Mn^{2+} binding in rat liver mitochondria with and without prior incubation with respiratory inhibitors. In both cases, ε^* is half-maximal at a total Mn^{2+} concentration of about 8 nmoles/mg protein. The midpoint concentrations in several similar experiments ranged between 5 and 10 nmoles/mg protein. However, the number of high-affinity binding sites is given not by the midpoint value, but by the total $[Mn^{2+}]$ at which ε^* begins to fall off from the plateau level (ε_b = 10–12). According to Fig. 2, this occurs at concentrations of about 2–4 nmoles/mg protein. Although this number is slightly lower than the reported number of high-affinity Fe^{3+} binding sites in rat liver mitochondria [31, 32], it is also close to that reported by Reynafarje and Lehninger [7] for the number of high-affinity Ca^{2+} binding sites. Consequently, these are probably the same high-affinity sites. First, the plateau limits for ε_b and free $Mn(H_2O)_6^{2+}$ concentration do not coincide (Fig. 2). Extrapolation of free $[Mn^{2+}]$ to zero reveals an abscissa intercept at $\approx$ 4 nmoles/mg protein, which approximates the number of binding sites, and is also a measure of their binding affinity (Fig. 2).

While the experiments of Figs 1 and 2 suggest that ε^* observed upon addition of Mn^{2+} to rat liver mitochondria reflect high-affinity binding, they only indirectly suggest a link between high-affinity binding sites and the energy-dependent divalent cation (M^{2+}) carrier. Fig. 3 compares the initial ε^* with the initial velocity of Mn^{2+} uptake in rat liver mitochondria, at several different temperatures and protein concentrations. In any case, a linear correlation between ε^* and uptake velocity is observed. The high-affinity binding sites, therefore, appear to be intimately involved

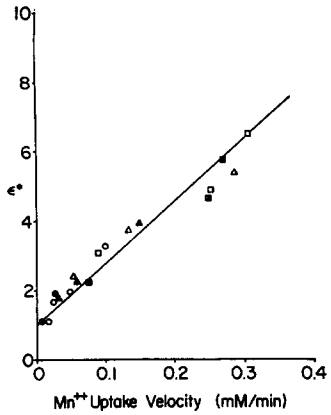

Fig. 3. Correlation between initial ε^* and Mn^{2+} uptake in rat liver mitochondria. Conditions as in Fig. 1B. Concentrations of mitochondrial protein ranged from 2 mg/ml to 40 mg/ml. The uptake velocity was determined from the initial slope of the decay in ε^*, relative to the difference between initial ε^* and ε^* at infinite time, and assumes that the extent of uptake is stoichiometric with the Mn^{2+} addition. (●), 0.0 °C; (○), 6.8 °C; (▲), 15.0 °C; (△), 19 °C; (■), 27.0 °C; (□), 38.0 °C.

with the divalent cation carrier, and ε^* ostensibly provides a tool for following both.

Effects of inhibitors and uncouplers

Incubation of mitochondria with antimycin and rotenone prior to the addition of Mn^{2+} has no effect on ε^* (Fig. 4), indicating that the respiratory inhibitors do not block binding of Mn^{2+} to the membrane components. If the duration of incubation is short, as in Fig. 4B, antimycin and rotenone do not influence the initial velocity of Mn^{2+} uptake. However, prolonged preincubation ($>$ 1 h at 0 °C and/or 5 min at 20 °C) results in only token uptake following the addition of Mn^{2+}. Nevertheless, the initial level of ε^* is as great as that in the control experiment (cf. Fig. 2). The persistence of Mn^{2+} uptake in the absence of respiration is consistent with the view that the divalent cation pump in mitochondria can utilize alternative energy sources [1–5] which are exhausted during the prolonged preincubation.

Several authors [4, 7, 31, 32] have presented evidence that addition of the uncouplers dinitrophenol and carbonylcyanide *m*-chlorophenylhydrazone (CCCP) eliminates the high-affinity Ca^{2+} and Fe^{3+} binding sites in mitochondria. Romslo and Flatmark [31, 32] have attributed these results to a conformational change accompanying "de-energization". The present results (Fig. 4C) indicate that the uncoupler FCCP, at a concentration of 0.2 nmole/mg protein, suppresses both the initial ε^* associated with Mn^{2+} binding and the steady-state of Mn^{2+} uptake. Scarpa and Azzone [4] and Reynafarje and Lehninger [7] have reported similar observations with high-affinity Ca^{2+} binding, but only at much higher uncoupler concentrations. If, as other workers have suggested [31, 32], "de-energization" of the inner mitochondrial membrane were to result in the concealment of high-affinity binding sites, the fall-off of ε^* in mitochondria which had been "de-energized" by incubation with antimycin and rotenone should have occurred at a much lower concentration of total Mn^{2+}. Evidently, the loss of high-affinity cation binding sites (Fig. 4C, also Refs 4, 7, 30, 31) is due to a special effect of uncouplers.

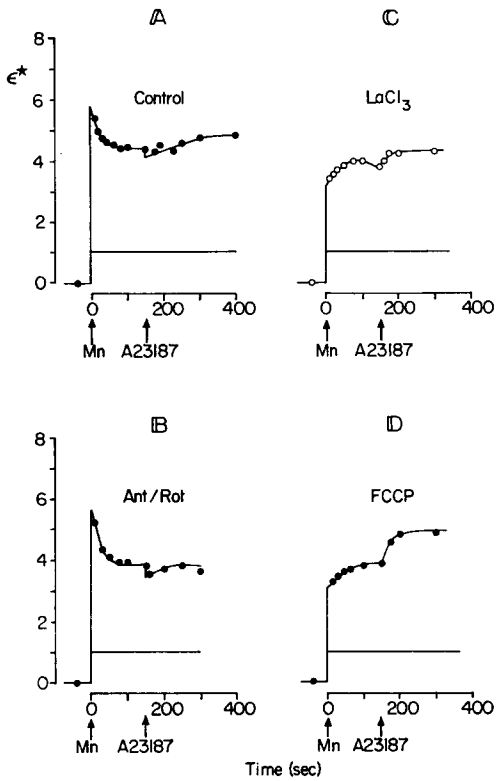

Fig. 4. Effects of respiratory inhibitors, uncouplers, and La^{3+} on ε^* and Mn^{2+} uptake in rat liver mitochondria. Conditions as in Fig. 1B, but with 10 mg mitochondrial protein/ml. 10 μM A23187 was added at a later time, as indicated. A. no additions made prior to addition of $MnCl_2$. B. 20 μg antimycin *a* and 1.5 μM rotenone present. Preincubation period was less than 5 min at 0 °C prior to the addition of $MnCl_2$. C. 100 μM $LaCl_3$ added prior to $MnCl_2$. D. 1 μM FCCP added prior to Mn^{2+}.

The effect of lanthanides on divalent cation transport in mitochondria is well known [4, 6]. Fig. 1D shows that La^{3+}, like uncouplers, not only retards Mn^{2+} uptake, but also reduces the initial level of ε^*. Separate measurements of ε^* in which Gd^{3+} is used as the paramagnetic probe in place of Mn^{2+} give results similar to Fig. 2, suggesting that lanthanides bind to similar high-affinity sites, as do Ca^{2+} and Mn^{2+}. Additional evidence also suggests that Gd^{3+} binding to mitochondria is also sensitive to uncouplers. The presence of 0.2 nmoles FCCP/mg protein causes the initial level of ε^* to fall from 5.3 to 1.4; hence, the uncoupler effect on Gd^{3+} binding and transport is stunning. Furthermore, since high-affinity sites are present in lipid-depleted mitochondria (Scarpa, A., unpublished), the high-affinity sites would appear to be associated with non-lipid components of the inner mitochondrial membrane.

Previous studies with lanthanides [4, 7] have revealed a number of inhibitor-sensitive transport sites which is an order of magnitude less than the number of high-affinity binding sites reported by Reynafarje and Lehninger [7]. At the same time, Scarpa and Azzone [4] have reported that lanthanide concentrations equal to the

number of high-affinity sites [7] lead to significant inhibition of Ca^{2+} efflux from mitochondria. The present study confirms these results, that at least ten times as much lanthanide is required to block efflux as to block uptake. Recent studies of the kinetics of mitochondrial calcium uptake [8, 29] have indicated that uptake is cooperative, requiring at least two divalent cations in the same vicinity in order to elicit energy-dependent transport. It is quite possible that divalent cation efflux from mitochondria proceeds by a mechanism involving the "carrier". If so, one must rationalize the differential sensitivities of Ca^{2+} uptake and efflux to lanthanides.

Structural and mechanistic properties of the carrier

If one adds Mn^{2+} to a suspension of mitochondria under limited loading conditions, the $g = 2$ sextet EPR spectrum of $Mn(H_2O)_6$ disappears completely. In its place, one observes a broad featureless spectrum with a band width of at least 1200 gauss at half-maximal amplitude. Ordinarily, one might attribute the annihilation of an Mn(II) EPR spectrum to a distortion of the ligand field as Mn^{2+} becomes bound, leading to a change in the electron spin relaxation time τ_s [33]. Previous work has established τ_s in the vicinity of 5 ns for $Mn(H_2O)_6$, but this number could be as long as 30 ns at room temperature [13, 14, 34].

Binding of Mn^{2+} to the inner mitochondrial membrane may or may not alter τ_s, but it should certainly increase the rotational relaxation time τ_r by several orders of magnitude. It might also change the ligand residence time τ_m, although this is less likely [14]. All three processes contribute to the correlation time for free (τ_c) or for bound (τ_b) Mn^{2+}. By assuming that the logarithm of the correlation time is inversely proportional to the absolute temperature [11, 13, 14, 34], one can estimate τ_b from water proton relaxation measurements according to the Solomon-Bloembergen equation [11, 13, 14]:

$$\frac{1}{T_{1M}} \approx A\left(\frac{3\tau_b}{1+\omega_I^2\tau_b^2} + \cdots\right) + \cdots \tag{3}$$

where A is a function of (distance)$^{-6}$, and $\omega_I = 2\pi$ times the radiofrequency.

Fig. 5 shows the effect of temperature and NMR frequency on the limiting enhancement ε_b. In this experiment, $1/T_{1p}$ and ε^* are determined at several protein concentrations and extrapolated to infinite protein. Since only trivial differences in the temperature curves for $1/T_{1p}$ and ε_b are apparent, the two parameters are considered interchangeable and do not show different temperature profiles. In each case, at every NMR frequency, ε_b first increases with temperature, then reaches a maximum, and falls off. At the maxima, $(\partial\varepsilon_b/\partial\tau_b) = 0$, and $\omega_I\tau_b = 1$, so that the correlation time can be calculated directly. Between 10 °C and 40 °C, τ_b ranges between 20 ns and 4 ns. This corresponds to an activation energy of 13 kcal/mole, which is identical to the activation energies for antimycin-induced Ca^{2+} efflux and A23187-mediated efflux of Mn^{2+} from rat liver mitochondria (Fig. 6).

For metal ions such as Mn^{2+} and Gd^{3+}, the correlation time is essentially equal to τ_r, because proton relaxation enhancements can be observed [11, 13, 14, 34]. The limiting condition for enhancement is $\tau_s \gg \tau_r$ and $T_{1M} \gg \tau_m$; hence, τ_s and τ_m fix the maximum limit of τ_r which can be measured by this technique. Whether this limit is reached in the case of carrier-bound Mn(II) in mitochondria thus becomes a relevant question. The observed correlation times (Fig. 5) are of the same order of

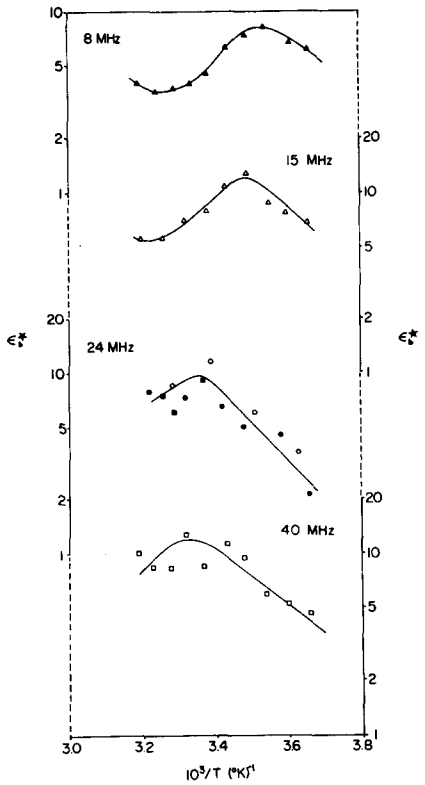

Fig. 5. Temperature and NMR frequency dependence of ε^* in rat liver mitochondria. Conditions as in Figs 1 and 3. ε_b^* is the limiting enhancement, determined by extrapolating ε^* to infinite protein concentration. Ordinate scales are logarithmic: (▲), NMR frequency is 8 MHz; (△), 15.0 MHz; (●, ○, ■), 24.3 MHz, separate experiments; (□), 40.0 MHz.

magnitude as τ_s for $Mn(H_2O)_6^{2+}$, and not very different from τ_m for the same species [13, 14].

The contribution of τ_r to τ_b can be estimated from the activation energies as well as from plots of T_{1p} versus ω_1^2 [11, 13, 14, 33]. At 4.5 °C, the data of Fig. 5 give a straight line at frequencies up to 24 MHz with an intercept at $\tau_b \approx 11$ ns, in reasonable agreement with data obtained directly from the "humps" in Fig. 5. However, the slope levels off as one increases the frequency. The reason for this phenomenon is not presently clear. The one condition which could generate such a curve ($\omega_1 \approx 0.01$ τ_b) does not hold in this case [13, 14]. Furthermore, the direction of the "curvature" is contrary to that expected for the frequency dependence of τ_s [13, 14]. On the other hand, at temperatures above 30 °C, the relation of T_{1p} versus ω_1^2 shows distinct hyperbolic character indicating a strong influence of τ_s. These results show that while τ_s is an important factor in τ_b, it does not necessarily dominate, especially at the lower temperatures. Evidently, the rotational diffusion time τ_r is observable for the Mn(II) carrier complex in mitochondria under such conditions.

Recent work with soluble proteins [11, 14] has revealed magnetic-field dependent correlation times similar to those observed above at temperatures above 30 °C.

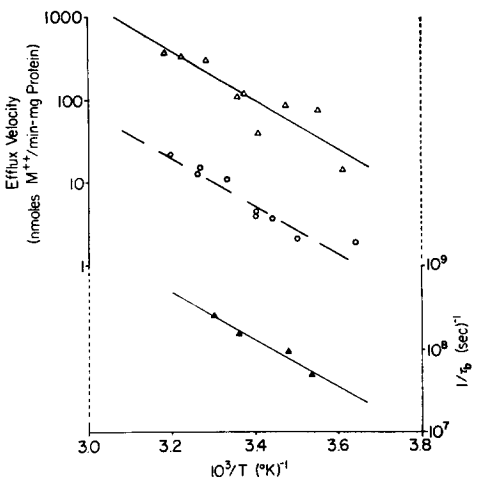

Fig. 6. Arrhenius plots of M^{2+} efflux and the temperature dependence of τ_b for the M^{2+} carrier in rat liver mitochondria. Mitochondria were suspended in the medium described in Fig. 1. Initial velocities of Ca^{2+} efflux induced by antimycin/rotenone (○) and Mn^{2+} efflux induced by A23187 (△) were measured spectrophotometrically [27] with 50 μM and 100 μM murexide, respectively, and 0.8 and 1.0 mg protein/ml respectively. 50 μM Ca^{2+} or Mn^{2+} was added to the suspension, and cation uptake was allowed to proceed to completion. Then either 0.9 mg/ml antimycin and 1.5 μM rotenone (○), or 2 μM A23187 (△) was added in order to elicit M^{2+} efflux. Correlation times of the carrier complex (▲) were obtained from the data of Fig. 5. Conditions as in Figs 1, 3, and 5. Both ordinate scales are logarithmic.

Further measurements [14] have shown that τ_m for Mn^{2+} changes from 27 ns to 5 ns as the ion becomes bound to pyruvate kinase, but that the 7 kcal/mole activation energy for H_2O exchange remains essentially constant. The present observations of 13 kcal/mole activation energy (Fig. 6) would argue that $\tau_m \gg \tau_b$.

The coincidence in activation energies for Mn(II)–carrier motion, antimycin-induced Ca^{2+} efflux, and ionophore-mediated Mn^{2+} efflux (Fig. 6) suggests that a common force is rate-determining for these transport processes. According to previous work [35], the mechanical resistance of the inner mitochondrial membrane is effectively 50 times the viscosity of water, and that τ_r for A23187 is approx. 15 ns at room temperature. In that case, the 11 ns correlation time for carrier-bound Mn(II) is much too short to represent the motion of a spherical Mn(II)–protein complex in the membrane (cf. ref. 14). However, it is consistent with a model in which Mn^{2+} is bound to a small, freely swinging molecular appendage whose size is comparable to that of the ionophore A23187.

Fig. 7 compares the temperature dependence of Mn^{2+} uptake kinetics in rat liver mitochondria measured spectrophotometrically (in collaboration with Drs J. M. Vanderkooi and A. Scarpa) and also by proton relaxation enhancement. Curvilinear Arrhenius plots are observed in either case, with an activation energy somewhere between extremes of 5 and 20 Kcal/mole. Similar activation energies have been reported for succinate metabolism by rat liver mitochondria, with a change in slope occurring in the vicinity of 25 °C [36]. Lee and Gear [37] have recently reported a substantially different temperature dependence for Ca^{2+} uptake driven by ATP

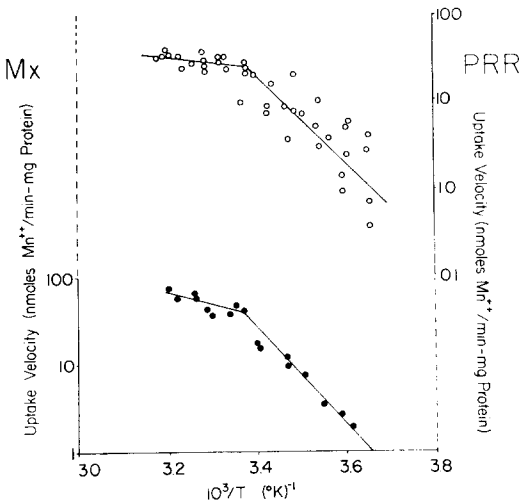

Fig. 7. Arrhenius plots of Mn^{2+} uptake in rat liver mitochondria. Initial velocities were determined either spectrophotometrically (●), or from the decay of ε^* (○). In the former case, conditions are same as for open triangles in Fig. 7. In the latter case, conditions as in Figs 1, 3 and 6.

hydrolysis, on the other hand. Apparently, Mn^{2+} uptake in mitochondria is rate-limited by whatever processes restrict energization, instead of those which merely limit molecular motion.

In the determination of Mn^{2+}-uptake velocities from ε^* measurements, one has to assume a value for the maximal extent of uptake. If uptake is essentially stoichiometric [2, 5, 26], then the velocities in Figs 3 and 7 are quantitatively accurate. On the other hand, if a constant fraction of the added Mn^{2+} is eventually transported (e.g. $\frac{1}{2}$), then the actual uptake velocities are systematically lower than indicated on the figures by that factor. In any case, the linearity of the plot in Fig. 3, and the slopes in Fig. 7 would not be affected. The good agreement in the temperature dependence of Mn^{2+} uptake between the two methods strongly suggests that, indeed, a constant proportion of the Mn^{2+} becomes bound to the high-affinity membrane sites and is taken up, regardless of the concentration of protein or free Mn^{2+} (cf. ref. 8,29). The results of Figs 6 and 7 would also indicate that, at temperatures below $\approx$ 25 °C, ε^* is a direct measure of carrier mobility. Hence, a direct correlation between the initial level of ε^* and the initial uptake velocity would suggest that the mobility of the carrier in fact determines the uptake velocity. One can then explain how the Arrhenius plots of energy driven uptake (Fig. 7 and Refs 36, 37) reveal the activation energy for energization, and not for the actual transport process.

The experiments of Figs 6 and 7 also allow a calculation of the number of water molecules coordinated to Mn^{II} bound to the divalent cation carrier. Given the coordination number and correlation time for $Mn(H_2O)_6$ [11, 12, 33], the present data indicate that for $\varepsilon_b = 11$, two H_2O molecules can remain attached to the Mn^{II} ion when it becomes bound to the inner mitochondrial membrane, giving [Mn^{II}(carrier)$(H_2O)_2$].

The presence of two coordination H_2O molecules in the Mn^{II}–carrier complex

TABLE II

EFFECT OF LIGANDS ON ε^* AND Mn(II) UPTAKE

Rat liver mitochondria were suspended in a medium containing 0.3 M mannitol and 0.05 M sodium morpholinopropanesulfonate with 4 mM sodium glutamate and 8 mM sodium succinate, pH 7.2. Final protein, 15 mg/ml. Conditions otherwise as in Figs 1, 3, and 4, except that the NMR frequency was 8.137 MHz. Where applicable, 10 mM phosphate buffer (pH 7.2) or 10 mM $K_2C_2O_4$ was present prior to the addition of 100 μM $MnCl_2$. Solutions of MnADP and MnATP were prepared immediately before addition to the mitochondrial suspension and the final ratio of nucleotide to total Mn(II) was 2:1.

Complex	Initial ε^*	Decay in ε^*	Standard* $1/T_{1p}$ (s)
$Mn(H_2O)_6^{2+}$	12.6	+	0.8
	12.0	+	
$Mn(C_2O_4)$	7.2	+	1.2
	6.3	+	
$Mn(HPO_4)$	5.9	+	1.6
	5.0	+	
Mn ADP^-	$\geqslant 7.3$	?	2.0
Mn ATP^{2-}	$\geqslant 7.8$	?	2.2

* Standard $1/T_{1p}$ values taken for 100 μM solutions of the complex in medium containing no mitochondria. Initial ε^* values were calculated on the basis of $1/T_{1p}$ for $Mn(H_2O)_6^{2+}$ in order to minimize the influence of τ_c differences in the determination of the numbers of H_2O molecules in the first coordination sphere.

would suggest that prior complexation with a monodentate ligand or even a bidentate ligand should not necessarily interfere with binding of an M^{2+} ion to the mitochondrial membrane. However, partial dissociation of a tridentate or polydentate ligand must occur prior to binding and transport. Table II compares ε^* values (before uptake), for several Mn^{II} complexes. The presence of oxalate or phosphate results in an initial ε^* which is about one half that observed for aqueous Mn^{2+} bound to mitochondria. If one employs a higher ratio of $MnHPO_4$ to protein, ε^* is initially smaller than that given in Table II, and uptake subsequently elicits significant de-enhancement ($\varepsilon^* < 1$) (see ref. 2). The present observation suggests that the mitochondrial M^{2+} carrier does not recognize M^{2+} ions on the basis of electrostatic charge, since the prevailing complex $MnHPO_4$ or MnC_2O_4 has none.

Substitution of acetate for phosphate results in initial ε^* values which are the same as those observed in the absence of any permeant anion (Table II). EPR data [5] suggest that acetate does not displace coordination water from $Mn(H_2O)_6^{2+}$; therefore, the anion must penetrate the inner mitochondrial membrane by a separate pathway. Consequently, the similarity in ε^* to that for the free aqueous ion both before and after Mn^{2+} uptake is not surprising.

Table II also shows the results of similar ε^* measurements with Mn^{II}-adenine nucleotides. ε^* values for the binding of MnADP are initially somewhat lower than for $Mn(H_2O)_6^{2+}$. A decrease in ε^* corresponding to Mn^{II} uptake may occur with Mn^{II}-adenine nucleotides as it does with aqueous Mn^{2+}, but the kinetics in this case would be slower. One might attribute this observation to the dissociation of the MnATP or MnADP complex, and the subsequent uptake of a hydrated Mn^{II} species.

DISCUSSION

As long as a paramagnetic ion is not "hidden" from bulk H_2O, binding to an immovable ligand results in ε^*. There is no reason to suspect, a priori, that large values of ε^* due to Mn^{2+} binding, for instance, are the result of binding to a specific protein. Chapell et al. [2] assigned the high ε^* values to Mn^{2+} binding to mitochondrial proteins, and the lower ε^* values to the binding of Mn^{2+} to phospholipids. ε_b values between 10 and 15 are observed for high-affinity Mn^{2+} binding to other types of biological membranes, under conditions in which Mn^{2+} is not known to be actively transported (see Table III). Titration of ε^* in rabbit muscle sarcoplasmic reticulum reveals high-affinity Mn^{2+} binding sites which are stoichiometric with the Ca^{2+}-dependent ATPase [38, 39]. Similar ε^* measurements in mitochondrial preparations from *Saccharomyces cervisciae* and from blowfly flight muscle also show high-affinity binding, ostensibly to proteins which are not involved in M^{2+} transport (cf. Refs 19, 21).

On the other hand, large ε^* values do not necessarily indicate binding of a paramagnetic ion such as Mn^{2+} to protein groups, either. Titration of the effect is nearly always necessary to determine the identity of the binding site. Mn^{2+} binding to chromatophore membranes from photosynthetic bacteria results in $\varepsilon^* \approx 10$ to 15 (Table III), for a very high number of sites. First, chromatophore membranes contain a very high proportion of phosphatidyl serine and phosphatidyl glycerol [40], both anionic lipids. Contrarily, mitochondrial membranes contain mostly neutral phospholipids plus some cardiolipin [41]. Divalent and polyvalent cations presumably bind much more tightly to the phosphate groups of phosphatidyl serine and phosphatidyl glycerol than to "uncharged" phospholipids, so that in the latter case, the bound cation could be more mobile (hence lower ε^*). The invisibility of high-affinity M^{2+} binding to the phosphate groups of mitochondrial cardiolipin, which is an anionic phospholipid, is harder to explain. Perhaps these lipids might account for the lower-affinity M^{2+} binding sites [2, 7, 31, 32]. Because of the chemistry of these binding sites, however, ε^* can provide a method for discriminating high-affinity binding from low-affinity binding.

The association between high-affinity M^{2+} binding and the divalent cation carrier would appear to hold true in most mammalian and plant mitochondria.

TABLE III

MAXIMUM ENHANCEMENT VALUES IN VARIOUS BIOLOGICAL MEMBRANES

Conditions as in Fig. 2. No energy source was present for any of the preparations.

System	ε_b	Titration (mole/mole)		Reference
Blowfly mitochondria	11 ± 1	≈ 5–$10/10^6$ g		—
Yeast mitochondria	11 ± 1	—		—
Rat liver mitochondria	11 ± 2	5–$10/10^6$ g		—
Sarcoplasmic reticulum	10 ± 2	1 : 1	ATPase phosphoenzyme	38, 39
Rps. spheroides chromatophores	13 ± 2	1 : 1	anionic phospholipids	40

However, in mitochondria from lower organisms such as yeast or insects, the presence of low-affinity M^{2+} transport is revealing [19, 21]. Regardless of whether any high-affinity binding sites exist in these systems, there is absolutely no evidence suggesting that the sites are even remotely connected with the cation transport system. One can argue, on the other hand, that low-affinity binding sites are intimately involved in divalent cation transport. Certainly this seems to be the case in yeast and insect mitochondria, but questionable in avian and mammalian systems.

While phospholipids appear perfectly capable of low-affinity binding in all mitochondrial systems studied, one could also argue that the low-affinity binding sites associated with M^{2+} transport in yeast and insect mitochondria are located on some part of a membrane protein. In this case, one must assume that protein ligands are not favorably located; otherwise the binding sites would have a high affinity for divalent cations. Conceivably, the difference between low-affinity binding and high-affinity binding of a metal ion to the carrier might be as slight as a small change in protein structure which could influence the spatial positions of one or two ligand sites. Two lines of evidence certainly suggest that the Mn^{2+} carrier in mitochondria from higher organisms is intimately associated with a membrane protein. First, extraction of mitochondria with organic solvents does not reduce the level of high affinity M^{2+} binding (Scarpa, A. unpublished). Furthermore, proteolysis with Nagarse [22, 29] impairs both high-affinity Mn^{2+} binding and transport (Fig. 1A).

If the divalent cation carrier and the high-affinity binding sites are associated with membrane proteins in heart and liver mitochondria, then the present results suggest that the actual sites be on an appendage of the membrane substituent, and not on the main body of any protein. Since two M^{2+} ions are required for transport [8, 29], one ion might bind to a site near the main body of the protein while the other ion could bind to a site on the extremity. Conceivably, the outlying extreme of this molecular arm is more liable to proteolytic cleavage than is the less accessible remainder of the protein, so that digestion with a protease should eliminate M^{2+} transport entirely while only partly destroying the binding process. One might imagine M^{2+} transport as the result of the protein "arm" swinging across the inner mitochondrial membrane. Oesterhelt and Stoekenius [42] have proposed a similar mechanism for the photoisomerization of bacteriorhodopsin in *Halobacterium halobium*. Other studies [43–45] have amply demonstrated the ability of this protein to function as a proton pump in artificial and biological membranes. Conceivably, a "swinging arm" mechanism could be a widespread feature of cation translocation in biological membranes. The requirement of an activator substance would explain both the ability of biological systems to control ion flows, and the cooperativity phenomenon in M^{2+} transport [8, 26].

The specificity of the metal ion carrier in mitochondria has been studied extensively. The present report suggests that the binding of metal ions to this species is governed by the chemistry of the ligands rather than by electrostatic effects. This observation is supported by the ability of the carrier to bind (with or without further transport) $MnHPO_4$ which is neutral, and MnADP or MnATP which are anions, in addition to the aquo-cations. Evidence is mounting that this species can transport not only the alkali earth cations [1–5] and Mn^{2+} [1, 2], but also Fe^{3+} [31, 32]. Whether the same carrier is also responsible for the transport of lanthanides (this work, also ref. 46) appears uncertain. The inhibition of lanthanide binding and trans-

port by uncouplers is in line with the similar sensitivity observed for the binding and transport of Ca^{2+} [4, 7], Mn^{2+}, and Fe^{3+} [31, 32]. On the other hand, the persistence of lanthanide transport in mitochondria which lack an appropriate energy source or a functional Ca^{2+} or Mn^{2+} carrier, suggests either that lanthanide transport proceeds via a distinctly separate carrier, or that the uptake of lanthanide ions does not require the cooperative participation of a second ion (cf. ref. 8, 29). The observation that lanthanide inhibition of Ca^{2+} uptake in mitochondria is competitive [4] would argue against the existence of discreetly separate carrier systems for lanthanides and other metal ions.

The temperature effects on the kinetics of M^{2+} uptake, release, carrier mobility, and membrane fluidity, seem harder to explain in terms of any one mechanism. Based on changes in the slopes of Arrhenius plots for succinate metabolism, Raison et al. [36] proposed that mitochondrial lipids undergo a phase transition at temperatures in the neighborhood of 25 °C. However, their data do not allow one to discriminate between two discrete slopes and a curvilinear Arrhenius plot for succinate metabolism. More recently, Lee and Gear [37] have reported 2–3 different transition temperatures for the oxidation–reduction kinetics of the mitochondrial cytochromes. Presumably, these Arrhenius plots resemble Fig. 7. The same authors [37] also reported the temperature dependence of ATP-driven Ca^{2+} transport, and observed a curve which is quite different from that for respiration-driven Ca^{2+} uptake.

On the other hand, this author's previous studies [35] of A23187 rotation in rat liver mitochondria clearly reveal a phase transition in the environs of the chromophore at a temperature of about 23 °C. The present report demonstrates, to the contrary, that no break in the temperature dependence of A23187-mediated Mn^{2+} efflux occurs at any temperature between 0 °C and 40 °C. Does this mean that the mobility of an ionophore has no bearing whatever on its own activity? More likely, additional processes are involved in A23187-facilitated transport besides rotational mobility.

A similar paradox appears in various studies with sarcoplasmic reticulum membranes. Arrhenius plots of spin label motion [46] and X537A-mediated Ca^{2+} efflux [47] show a break in the vicinity of 20 °C. At the same time, measurements of A23187 rotation in sarcoplasmic reticulum [35] reveal no such phase transition since these Arrhenius plots are linear. Davis and Inesi [48] have further shown that throughout the temperature range of 0 °C to 40 °C, the phospholipids in sarcoplasmic reticulum exist as a 2-phase equilibrium mixture of solid and liquid. One can argue that at temperatures below a critical value, a sufficient portion of the membrane lipids should be "frozen" to restrict the motion of probes or membrane proteins.

Conceivably, the critical temperature would depend on the fraction of the total area of the membrane occupied by that component. In such a case, correlation of the break point temperatures between any two processes in the same membrane would be meaningless, since different membrane components have different sizes. And the absence of any break point in an Arrhenius plot (see Fig. 7) would indicate that the substance in the membrane is small enough to avoid being frozen out. On this basis, one could employ this argument to attribute a curvilinear Arrhenius plot [37] to the successive freezing out of electron transport particles in the mitochondrial membrane, based on size. The more massive particles would "freeze out" at higher temperatures, the smaller ones at lower temperatures. M^{2+} transport which is driven by electron transport would, of course, depend on the functional ability of the entire respiratory

chain, so that its temperature dependence should mimic that for all of the electron carriers, regardless of its own size. If the carrier possesses small-molecule mobility, one should expect the temperature dependence of M^{2+} uptake, driven by an alternative energy source, to be different from that shown in Fig. 7. It should reveal lower transition temperatures [37], or no transitions at all. In any case, the energy source should have no effect on the temperature dependence of M^{2+} efflux. On the other hand, these arguments cannot themselves account for the disagreement in the temperature dependence curves for A23187 mobility [35] and A23187-mediated Mn^{2+} efflux (Fig. 7).

The present data provide some insight into the physicochemical properties of the divalent cation carrier in mitochondria. While the identity of the carrier species in rat liver mitochondria could not be unambiguously determined from this work, some clues have emerged as to the structure of the high-affinity binding site. These results appear to narrow the possible mechanisms of metal ion transport in mitochondria to those which place the active binding site on a relatively mobile, small molecular weight portion of a membrane substituent.

ACKNOWLEDGEMENTS

The author wishes to thank Dr Richard Hansford for his generous donation of blowfly mitochondria and for stimulating discussions, and also Drs John S. Leigh, Jr and Antonio Scarpa for their valuable criticism of this manuscript. Further discussions with Drs George Reed, Tomoko Ohnishi, and Britton Chance also proved very helpful in this work. I also wish to thank Setsuko Shiraishi, Kathleen Strimell, and James Simmons for their expert technical assistance, and Barbara Payne and Kenneth Ray for help in the preparation of this manuscript. This work was supported by U.S. Public Health Service grant GM 12202 and postdoctoral fellowship GM 55536.

REFERENCES

1 Lehninger, A. L., Carafoli, E. and Rossi, C. S. (1967) Adv. Enzymol. 29, 259–320
2 Chappell, J. B., Cohn, M. and Greville, G. D. (1963) Energy Linked Functions of Mitochondria (Chance, B., ed.), pp. 219–231, Academic Press, New York
3 Brierley, G. P., Backman, E. and Green, D. E. (1962) Proc. Natl. Acad. Sci. U.S. 48, 1928–1935
4 Scarpa, A. and Azzone, G. F. (1970) Eur. J. Biochem. 12, 328–335
5 Puskin, J. S. and Gunter, T. E. (1973) Biochem. Biophys. Res. Commun. 51, 797–803
6 Mela, L. and Chance, B. (1969) Biochem. Biophys. Res. Commun. 35, 556–559
7 Reynafarje, B. and Lehninger, A. L. (1969) J. Biol. Chem. 244, 584–593
8 Vinogradov, A. and Scarpa, A. (1973) J. Biol. Chem. 248, 5527–5531
9 Gunter, T. E. and Puskin, J. S. (1972) Biophys. J. 12, 625–635
10 Puskin, J. S. and Gunter, T. E. (1972) Biochim. Biophys. Acta 275, 302–307
11 Mildvan, A. S. and Cohn, M. (1970) Adv. Enzymol. 33, 1–70
12 Leigh, J. S. (1970) J. Chem. Phys. 52, 2608–2612
13 Bloembergen, N. and Morgan, L. O. (1961) J. Chem. Phys. 34, 842–850
14 Reuben, J. and Cohn, M. (1970) J. Biol. Chem. 245, 6539–6546
15 Vieira, F. L., Shaafi, R. I. and Solomon, A. K. (1970) J. Gen. Physiol. 55, 451–466
16 Case, G. D. (1974) Fed. Proc. 33, 1399, Abstract 994
17 Reed, P. W. and Lardy, H. (1972) J. Biol. Chem. 247, 6970–6977

18 Wong, D. T., Wilkinson, J. R., Hamill, R. L. and Horng, J. S. (1973) Arch. Biochem. Biophys. 156, 578–585
19 Carafoli, E., Hansford, R. G., Saktor, B. and Lehninger, A. L. (1971) J. Biol. Chem. 246, 964–972
20 Vinogradov, A., Scarpa, A. and Chance, B. (1972) Arch. Biochem. Biophys. 152, 646–654
21 Balcavage, W. X., Lloyd, J. L., Mattoon, J. R., Ohnishi, T. and Scarpa, A. (1973) Biochim. Biophys. Acta 305, 41–51
22 Chance, B., and Hagihara, B. (1961) Proceedings, Fifth International Congress of Biochemistry, Moscow, Vol. 5, 3–33
23 McFarland, B. and Inesi, G. (1971) Arch. Biochem. Biophys. 145, 456–464
24 Jackson, J. B., Crofts, A. R. and von Stedingk, L. V. (1968) Eur. J. Biochem. 6, 41–54
25 Lindberg, O. and Ernester, L. (1957) Methods Biochem. Anal. 3, 1–22
26 Mela, L. and Chance, B. (1968) Biochemistry 7, 4059–4063
27 Scarpa, A. (1972) Methods Enzymol. 24, 343–351
28 Cohn, M. (1963) Biochemistry 2, 623–629
29 Scarpa, A. and Graziotti, P. (1973) J. Gen. Physiol. 62, 756–772
30 Hansford, R. G. and Chappell, J. B. (1967) Biochem. Biophys. Res. Commun. 27, 686–693
31 Romslo, I. and Flatmark, T. (1973) Biochim. Biophys. Acta 305, 29–40
32 Romslo, I. and Flatmark, T. (1973) Biochim. Biophys. Acta 325, 38–46
33 Carrington, A. and McLachlan, A. D. (1967) Introduction to Magnetic Resonance, J. Wiley Sons, New York
34 Reed, G. and Cohn, M. (1970) J. Biol. Chem. 245, 662–667
35 Case, G. D., Vanderkooi, J. M. and Scarpa, A. (1974) Arch. Biochem. Biophys. 162, 174–185
36 Raison, J. K., Lyons, J. M. and Thomson, W. W. (1971) Arch. Biochem. Biophys. 142, 83–90
37 Lee, M. P. and Gear, A. R. L. (1973) Abstracts, 57th FASEB Meeting, Atlantic City, N.J., April 15-20, p. 515
38 Makinose, M. (1969) Eur. J. Biochem. 10, 74–82
39 Inesi., G., Mering, E., Murphy, A. J. and McFarland, B. H. (1970) Arch. Biochem. Biophys. 138, 285–294
40 Haverkate, F., Tuelings, F. A. and van Deenen, L. L. M. (1965) K. Ned. Akad. Wet. Proc. B 68, 154–159
41 Fleischer, S., Rouser, G., Fleischer, B., Casu, A. and Kritchevsky, G. (1967) J. Lipid Res. 8, 170–180
42 Oesterhelt, D. and Stoekenius, W. (1973) Proc. Natl. Acad. Sci. U.S. 70, 2853–2857
43 Kayushin, L. P. and Skulachev, V. P. (1974) FEBS Lett. 39, 39–42
44 Drachev, L. A., Kaulen, A. D., Ostroumov, S. A. and Skulachev, V. P. (1974) FEBS Lett. 39, 43–45
45 Racker, E. and Stoekenius, W. (1974) J. Biol. Chem. 249, 662–663
46 Reed, K. C. and Bygrave, F. L. (1974) Biochem. J. 138, 239–252
47 Eletr, S. and Inesi, G. (1972) Biochim. Biophys. Acta 282, 174–179
48 Scarpa, A., Baldassare, J. and Inesi, G. (1972) J. Gen. Physiol. 60, 735–749
49 Davis, D. and Inesi, G. (1971) Biochim. Biophys. Acta 241, 1–8